#### **Research Article**

Mushtaq Talib Mezaal\*, Norazizah Binti Mohd Aripin, Noor Shamsiah Othman and Adheed Hasan Sallomi

# The effect of urban environment on large-scale path loss model's main parameters for mmWave 5G mobile network in Iraq

https://doi.org/10.1515/eng-2022-0601 received January 03, 2024; accepted February 15, 2024

**Abstract:** The high speeds resulting from the use of millimeter waves (mmWave) in 5G mobile networks are accompanied by high path loss. The issue of generating a reliable propagation model of radio waves is crucial to the development of cellular networks since it reveals essential information regarding the properties of the wireless channel. The received signal strength, the coverage area, and the outage probability in certain places may all be determined through theoretical or empirical radio frequency propagation models, which offer essential valuable information regarding signal path loss and fading. This work analyzes a comprehensive three-dimensional ray-tracing method at 28 GHz for Najaf city, Iraq. The optimum path loss model for the city of Najaf is evaluated using the close-in (CI) model. On average, the values of the main parameters of CI model n,  $X_{\sigma}^{\text{CI}}$  accomplished, respectively, 3.461866667 and 11.13958333. The lowest achievable path loss exponent was 3.0619 across all analyzed scenarios, while the highest possible value was 4.1253. The results of this work can serve as a baseline for mmWave measurement campaigns conducted in comparable conditions, and they provide a new avenue for future research into mmWave at 28 GHz in Iraq.

**Keywords:** mmWave, 5G, close-in model, PLE, shadow fading

Norazizah Binti Mohd Aripin, Noor Shamsiah Othman: Electrical and Electronics Department, Universiti Tenaga Nasional, Selangor, Malaysia Adheed Hasan Sallomi: Electrical Department, University of Mustansruyah, Baghdad, Iraq

## 1 Introduction

Due to the vast development in data consumption, communication infrastructure, mobile subscriptions, and the increasing penetration of mobile and Internet of Thing (IoT) devices, the needs for cellular bandwidth have been severely stretched. To overcome the constraints of the existing technology, the next generation of communication technology will need to enhance its spectral efficiency, expand its bandwidth, and develop better technology for recycling spectrum. The ultra-low latency and massive network capacity relayed to 5G mmWave communication, along with higher performance and ameliorated efficiency, promise a wide range of potential user applications. These applications include smart cities, the IoT, industrial automation, and vehicular communication. There are two key issues with millimeter waves (mmWave) that make it less than ideal for 5G: high path loss and high penetration losses. It has been justified that mmWave operate in extremely power-limited regimes, restricting the flexibility with which spatial antenna structure and expanded bandwidth freedom may be utilized [1]. The most suitable way to describe the signal attenuation of a transmitting and receiving antenna, depending on the separating distance between them furthermore some other parameters, is the path loss model [2]. The signal losses passing through a radio frequency channel can be predicted by using a suitable path loss model [2]. Short wavelengths of mmWave occur due to reflection, scattering, line-of-sight (LOS) propagation, diffraction, and penetration of materials, which will cause a large size of attenuation. Over the past few years, numerous companies and research groups have presented a wide range of scenarios to simulate various measurements and models [3,4]. Checking channel parameters is the cornerstone of the design of any millimeter wave transmission and receiving system. To check those parameters for each millimeter channel, there are two main methods: measurements and modeling. Several factors make it challenging to perform physical measurements completely, such as the high cost

<sup>\*</sup> Corresponding author: Mushtaq Talib Mezaal, Electrical and Electronics Department, Universiti Tenaga Nasional, Selangor, Malaysia, e-mail: pe21105@student.uniten.edu.my

and furthermore heavy weight of the measuring devices, in addition to the weather conditions specific to each place; therefore, path loss modeling is preferred over field measurement.

Ultimately, 5G aims to realize a highly adaptable radio access architecture capable of advocating extremely high volumes of machine-type communications. The critical loss, high path loss, and high absorption rate of 5G mmWave transmission through vegetation are all issues that have been identified. Chen [5] suggested working on a 5G diminutive cell mmWave technology operating at 28 GHz to address the limitations of 5G. Path loss modeling is essential for determining the best placement and coverage for mmWave network transmitter antennas. The problem of modeling path loss has been tackled from numerous angles, with several empirical, deterministic, and ANN-based models being produced. Network optimization engineers can benefit greatly from path loss prediction algorithms since they can utilize them to better place base stations, choose transmitting and receiving antennas, establish optimal operating frequencies, and do interference analyses. The presence of numerous criteria adopted in classifying the channel models has made it challenging to classify these models despite the great efforts made to do so [6]. The most common types of radio propagation models are empirical and deterministic. Diffraction principles [7], integral equations [8], ray tracing [9], and parabolic equations [10] form the theoretical foundation for deterministic models. Author in [11], the conventional propagation model [12], and the COST 231-Hata model [13] are all examples of empirical models that are based on driving test measurements of the target regions. These models require minutes in the way of computing resources, and they may be deployed quickly at minute cost. Their lack of adaptability to changing conditions means they are less reliable than other models. At 800 and 1,800 MHz, Cheerla et al. [14] utilized Newton's approach to generate an optimized COST 231-Walfisch-Ikegami (CWI) model. Using this strategy, they were able to validate the path loss prediction in the field with better precision than using the empirical CWI model. As a result, before launching a pilot study and building the expensive mmWave infrastructure, it is crucial to investigate the surrounding area and run through simulations. As a result, the primary objective of this study is to run a high-resolution, three-dimensional (3D) ray-tracing simulation of Najaf city, Iraq, at 28 GHz. For 28 GHz, the path loss is characterized by the close-in (CI), alpha-beta-gamma (ABG), and floating intercept models, depending on the height difference between the transmitter and receiving antennas (30 vs 2 m). These models fall into one of three categories that Erunkulu [2] established based on the carrier frequencies. Although there are numerous types of path loss models, all path loss

models do not exactly satisfy the Iraqi conditions as demonstrated in the study of Al-shuwaili [15]. Al-shuwaili [15] and Jamel [16] simulated 5G network for Baghdad city by studying the impact of the weather conditions furthermore the suitable mmWave band for Iraq, while neglecting at the same time the impact of the other essential elements like the urban distribution that distinguishes a city from another.

This article provides a detailed path loss study at 28 GHz utilizing the CI path loss model at a  $T_x/R_x$  height of 30–35/1.5 m. Before embarking on 5G network planning, academics and service providers can utilize the findings from this work as a baseline for their own research in a comparable scenario. The purpose of this research is to refine the existing path loss model at 28 GHz so that it better accounts for the dense urban environment of Najaf city. This article's goals are to first examine the impact of path loss on a citywide scale in Najaf at 28 GHz mmWave using four distinct base station (BTs) sites and provide the results of those analyses. In addition, the path loss exponent (PLE) and shadow factor must be determined as a result of this work.

This study provides contributions including utilizing intelligent ray-tracing simulation provided by FEKO-WinProp software to generate a novel deterministic path loss model at 28 GHz for the city of Najaf, Iraq. In addition, the parameters of the suggested path loss model, including the PLE, the shadow factor, and the random Gaussian standard deviation, have been fine-tuned to the target environment. Furthermore, the optimal model to reflect path loss in a 28 GHz environment has been determined by computing CI path loss model for a range of scenarios based on the special location of the transmitter. In conclusion, the results gained in this work may be utilized as a standard for future efforts in research on Najaf city and the other surrounding provinces which share the same environment.

### 2 Related works

The mmWave utilized in 5G networks is closely related to path losses and absorption losses. Conversely, the communication between the transmitter and receiver in the two environments (LoS and non-line-of-sight [NLoS]) can be established based on the phenomena of reflection and scattering. Several factors limit the free space accomplished by the mmWave spectrum, including the molecular size of raindrops, as well, due to the short length of mmWave [2]. Temperature and humidity moreover have a significant impact on the mmWave by absorbing part of the signal energy, causing it to be attenuated. mmWave at

higher frequencies suffers from higher attenuation over distance. Absorption losses due to oxygen furthermore other environmental factors have been studied by Rappaport et al. [17]. Attenuation is an additional effect on the propagation channel that occurs due to excess path loss. Increasing the size of the transmitter or receiver antenna can exceed the mmWave path loss. The effective surface of each antenna is the primary determinant of each antenna gain, which in turn determines the permissible path limits. In the case of the LoS mmWave channel, the boresight alignment controls the occurrence of effective communication with the directional antenna, so the parameters associated with the antenna (such as the antenna position, location, and pattern) affect the quality of communication as they either mitigate or increase path losses [18]. To mitigate path losses, the transmitter must be physically directed toward the receiver in the case of antennas with fixed beam patterns. To accomplish effective communication in the case of NLoS communication channels, the antenna inside the single beam must be directed toward one or more reflections, provided that the reflection is dominant. One of the conditions for the NLoS channel to be the best is when a complicated beam pattern is available, which can divide the energy over multiple propagation paths. The antennas utilized with the NLoS channel must have some adaptation to accomplish the best NLoS channel. Several characteristics must be provided in future antennas utilized for mmWave such as antenna gain, beamwidth, and beam pointing technique to mitigate the effect of interference on communication quality [18].

The path loss prediction can be defined as the possibility of determining the effect of attenuation with an acceptable level of accuracy on the propagation of radio signals. Path loss prediction is considered one of the basics in any planning process for establishing a wireless communication network [19]. To determine propagation losses for a specific network, accurate data between the transmitting and receiving stations must be generated through widefield campaigns to measure the received signal strength (RSS) [20-22]. A model for predicting path losses has been proposed by Al-samman et al. [23], which is devoted to finding path losses in 5G mmWave and future 6 GHz communications by inserting a frequency-dependent attenuation factor. To solve multi-task missions related to direct and multi-hop communication applications, Elizabeth et al. utilized an unmanned aerial vehicle (UAV) to discover which path is the fastest [24]. They concluded that the propagation signal strength could be enhanced prior to the deployment of network infrastructure by relying on multiple UAVs [24]. Authors in [25] justified the dependence of the path loss distribution on the general environmental characteristics of the target area. Three categorized propagation environments are urban, suburban, aquatic, tunnel, furthermore rural, on which the path loss value depends on which it is most closely relied for estimating PLE. For urban environments, the path loss can be estimated to be 30-50 dB, depending on the height and type of building materials. The path loss generated by ground terrain per 1 km can be estimated at 90 dB [26]. For aquatic environments, Sasidhar [27] estimated the path losses due to the surfaces of oceans and seas; Hrovat et al. [28] investigated the path losses in the tunnels utilized for metro and trains due to obstacles and traffic in the roads and railway tunnel, which leads to an increase in the propagation signal's delay spread. Besides poor communication quality in the tunnel environment, additional path losses can be recorded due to objects moving inside the tunnels [28]. Cellular coverage can be practically predicted by relying on geometric mathematical models for ray tracing through computer simulations. Researchers resort to using a high computer to predict the coverage of any cellular system due to the high costs associated with the drive test furthermore to save time as well. For these reasons, numerous companies have adopted several 3D modeling software developed to meet a variety of work. Propagation simulation modeling using ray tracing and drive test measurement campaigns are the two main types of modeling for calculating path losses. The propagation characteristics are measured in drive test campaigns using advanced measuring software and tools.

Ray-tracing techniques have recently expanded to include path loss prediction models based on artificial intelligence techniques such as convolutional neural network (CNN) and artificial neural network (ANN), by integrating two-dimensional (2D) satellite images with 3D models to generate a general method for predicting path losses [29,30]. Several elements control the accuracy of 3D digital maps, such as terrain, foliage, and city buildings, in addition to other features such as the location of the transceivers, building edges, street features, and facades. 3D ray-tracing simulation models can flexibly alter some parameters that are impossible to adjust furthermore calibrate during field first-hand practice. High computational complexity combined with long simulation time is the only drawback of using 3D ray tracing. The CNN-based 2D satellite image was utilized by Ahmadien et al. [29] to overcome the high computational complexity required for 3D raytracing simulation. Ahmadien et al. [29] discussed the possibility of predicting the path losses for the transmitting and receiving antennas at various heights and various frequencies. Relying on CNNs, Ates et al. [31] presented a deep learning model with an accuracy of 88 and 76% for PLE and large-scale shadowing factor, respectively. The model was trained and tested by 3D ray tracing after extracting pertinent properties found in 2D satellite images. The deep neural network utilizes a 2D satellite image as input to begin the process of predicting channel parameters. For a successful and effective deeplearning model, huge data are required for the purpose of training and testing. To obtain these huge data, 3D ray-tracing simulation is utilized to generate it within the study area based on the propagation modeling software [32]. To model path losses, some researchers [32] have introduced 3D raytracing to accomplish their goal. To study the wave propagation between an LTE base station and a vehicle, Charitos et al. [33] relied on 3D ray tracing for the purpose of predicting the spatial and temporal multipath ray components in their article [33]. The authors compared the results obtained by simulation with realistic measurements taken with a drive test of the target area. The authors demonstrated the ability of the virtual drive test to produce results with higher accuracy and reliability than the measured value. Path loss models have been modeled by Thrane et al. by ray tracing using deep-learning techniques furthermore made use of satellite images and drive tests [34]. The authors demonstrate a significant improvement in path loss prediction for models developed with deep-learning techniques, scoring 1 dB for 811 MHz networks and 4.7 dB for 2630 MHz networks. An extensive review of path loss models based on the ray-tracing model has been presented by Thrane et al. [34]. The focus of the review was on the accuracy obtained for path losses based on 3D tracing techniques for outdoor propagation scenarios. The authors conclude that there is a certain level of uncertainty in ray-tracing models resulting from the utilization of numerical maps, although they insist that raytracing models remain the best predictors of path losses, neglecting at the same time the high computational requirements. A new dual regression model has been proposed by Han et al. utilizing Network Simulator Version 2 (NS-2) that provides the transmitter and receiver freedom of movement without sudden alters in the correlated space path loss [35]. The authors' main objective is to break down the difficulties associated with the movement of both the transmitter and the receiver by constructing a spatially correlated path loss for a mobile-to-mobile simulation. The authors utilized drive test campaigns to validate the accuracy of the results obtained from the proposed model that advocates the maintenance of spatial correlation related to path losses for both indoor and outdoor scenarios. One of the most crucial factors limiting the performance of wireless communication networks that operate using mmWave is the losses that occur as a result of atmospheric absorption, in addition to the path losses [36]. In New York City, Maccartney et al. launched an extensive campaign measuring mmWave propagation at frequencies of 28 and 73 GHz [37]. The study demonstrated by comparison that novel large-scale path loss models are better in terms of adaptation

and performance relative to 3rd generation partnership project and international telecommunication union (ITU) propagation models. Sun et al. [38] demonstrated, regarding the accuracy of prediction for 5G networks operating in mmWave, that the well-known ABG model predicted less than acceptable levels for regions near the transmitting antenna while it over-predicted for regions far from transmitter antenna. The results indicate that the CI and close-in free space models provide better computational simplicity. Rappaport et al. [17] justified through extensive measurement campaigns within the city of New York the relationship of the value of the PLE with the dense urban environment of the city furthermore its recording of higher values. It is possible to propose a new path loss model based on the measurements obtained through the extensive propagation measurement. This proposed model can predict path losses furthermore and relate them as a function between distance and transmitter frequency for the indoor and outdoor scenarios. Bhuvaneshwari et al. [39] combined ray-tracing with the Walfisch-Ikegami model to provide a hybrid model with a better ability to predict path losses. The hybrid model accomplished 69.9% less error. The results obtained from the hybrid model were verified by a field campaign of measurements for GSM networks with a frequency of 900 MHz in Hyderabad, India. The CI model was developed by Batalha et al. based on measurements obtained from campaigns in the indoor environment at mmWave frequencies, and measurements are normalized by the minimum mean square error (MMSE) technique [40]. In the published paper [41] for an indoor environment, specifically a diminutive office, an assessment of mmWave propagation was done utilizing a 3D ray-tracing model. Models like COST-WI allow for performance validation of the simulation model with real-world field measurement in an urban setting. Due to COST-WI considering realistic environmental factors like road width, building elevations, street alignments, and vegetation, it can only be utilized in certain contexts. Moreover, COST-231 [13] is another alternative. A comprehensive mmWave frequency indoor measuring campaign was carried out by the author in ref. [40]. The least mean square error (MMSE) technique was applied to field measurement data to generate a path loss adjusting model for a near-field path loss model under LoS and NLoS environments. The author proposes a 3D ray-tracing model to simulate the path loss at 28 GHz in an indoor setting (Tables 1 and 2).

# 3 Experimental setup and data collection

Using a 3D map of Najaf city, Iraq, we provide a large-scale path loss model at 28 GHz, with study area coordinates of

Table 1: Summary of recorded parameters of CI path loss model in various countries

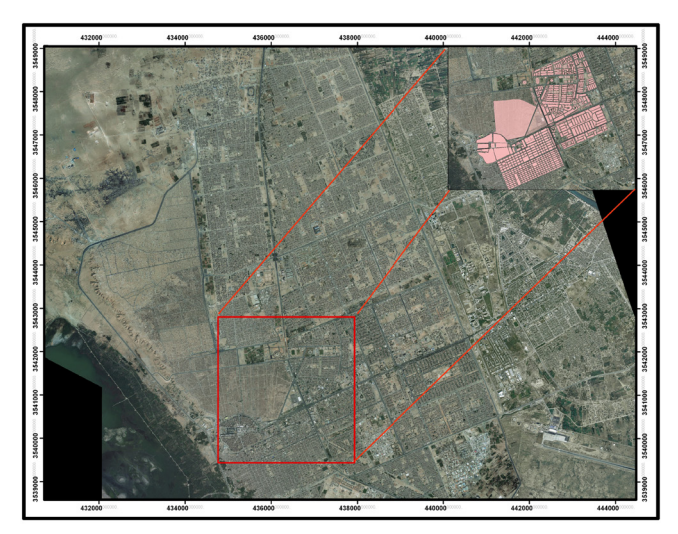
No.	Reference	Utilized frequency in GHz	$X^{ ext{CI}}_{\sigma}$	n	Model type	Country
1	[37]	28	2.5–10.8	1.7–5.1	Empirical	USA
		73	3.2-15.9	1.6-6.4	·	
2	[38]	38	5.3	2.9	Empirical	USA
		73	8	3.2		
3	[42]	19	_	0.6	Empirical	UK
		28	_	0.6		
		38	_	1.3		
4	[43]	28	8.36	3.73	Empirical	UK
		38	5.78	3.88		
5	[20]	3.5	6.54, 6.97	1.48, 1.95	Empirical	Malaysia
			5.91, 7.44	1.32, 1.78		
6	[44]	3.5	6.98, 7.73, 4.99	1.98, 2.07, 1.94	Empirical	Malaysia
			4.89, 5.91, 3.50	1.82, 1.99, 1.76		
7	[45]	28	4, 2.6	2	Empirical	China
		38	2.3, 1.8	2		
8	[46]	40	4.7, 9	1.8, 2.9	Empirical	USA
9	[47]	60	_	1.56-1.78	Empirical	South Korea
				3.87		
10	[41]	28	3.6	2.1	Empirical	Malaysia
		38	2.4-3.6	1.8, 1.9, 2		
		78	4.2-5.2	2		
11	[18]	28	34.72, 52.21	1.46, 2.19	Empirical	Nigeria
			52.32, 71.63, 71.52	2.2, 3, 3.01, 3.9		
12	[15]	28	_	2	Empirical	Iraq
13	[16]	28	_	2	Empirical	Iraq
		73	_	2		

435,000, 3,542,000 to 438,000, 3,540,000. Since the 28 GHz carrier frequency offers a reasonable compromise between the detrimental effects of factors including path loss, rain fading, propagation loss, transmission via vegetation loss, and the atmospheric absorption effect, it was chosen as the optimal frequency. South Korea, Malaysia, the United Kingdom, the United States, China, and Japan have all tested and deployed this frequency range in the outdoors [56]. The carrier frequency of 28 GHz is optimal for tiny cells that operate over short distances, allowing for excellent data

throughput [3]. In Figure 1, we see both a 3D map and a satellite image of the area under investigation. Our research region is labeled by the red polygon of 435,000, 3,542,000 to 438,000, 3,540,000. The block diagram of the simulation is illustrated in Figure 2. Obtaining the spatial maps of Najaf city is the initial part of our methodology. The spatial maps are obtained from the geographic information system (GIS) center of Najaf. Najaf databases include the spatial maps of each residential quarter beside any other buildings available in the targeted zone. The provided maps by the GIS

Table 2: Summary of related works on ray tracing model

No.	Reference	Frequency in GHz	Environment	Antenna	Model	Model type
1	[48]	28	Open square – NLOS	_	Ray tracing	Deterministic
2	[40]	3.5	Indoor-LOS & NLOS	Omnidirectional	Ray tracing	Deterministic
3	[49]	28	Open square-LOS and NLOS	_	Ray tracing	Deterministic
4	[50]	28	Urban – LOS	Isotropic	Ray tracing	Deterministic
5	[51]	28	Indoor-LOS and NLOS	Omnidirectional	Ray tracing	Deterministic
6	[52]	28	Outdoor-LOS and NLOS	Omnidirectional	Ray tracing	Deterministic
7	[53]	28	Indoor-LOS and NLOS	Empirical horn 3D-directional	Empirical and ray tracing	Deterministic
8	[54]	28	Outdoor-LOS and NLOS		Ray tracing	Deterministic
10	[55]	5, 30, and 60	Outdoor, Indoor-NLOS	Directive antenna	Dominate path model	Deterministic



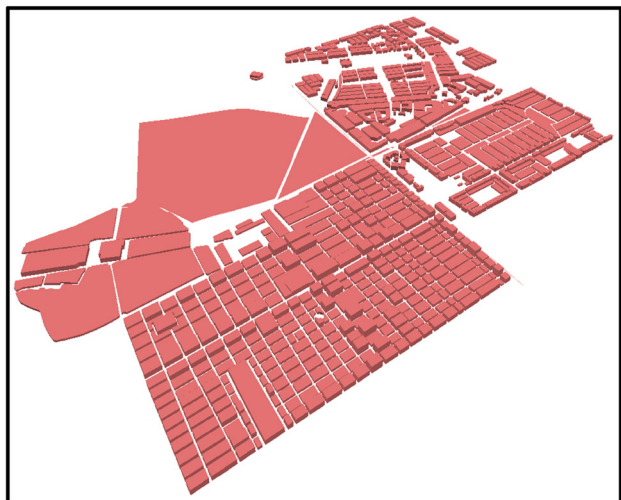


Figure 1: The targeted area of the study is in both 2D and 3D views.

center are in 2D, and for our work it needs to be converted in 3D to describe each building height in the tagged zone. Using WinProp WallMan software [57], the spatial maps are going to be simplified. Each building that appears in the targeted zone will obtain its real elevation above the ground to simulate the real urban environment of the city. For simulation, a single-layer dielectric of ITU concrete 28 GHz type was considered for construction appears in the map. Based on the provided data by the Communication and Media Commission, a government institution concerned with regulating media and communications in Iraq, the base stations for one of the well-known service providers

in Iraq Zain Company will be utilized during the simulation as demonstrated in Figure 3. After deploying the towers, all parameters regarding each transmitter available in the base station and the receiver will be set as illustrated in Table 3.

Since Iraq is like numerous other countries that have not upgraded yet to 5G furthermore still works with 4G. Therefore, it is impossible to obtain real measurements for 5G networks. A very interesting feature provided by WinProp software is executing virtual drive tests [58–60]. This feature is so useful to our work due to the lack of real measurements for 5G networks in Iraq. After executing the virtual drive test, the received power value for each  $T_{\rm x}$ 

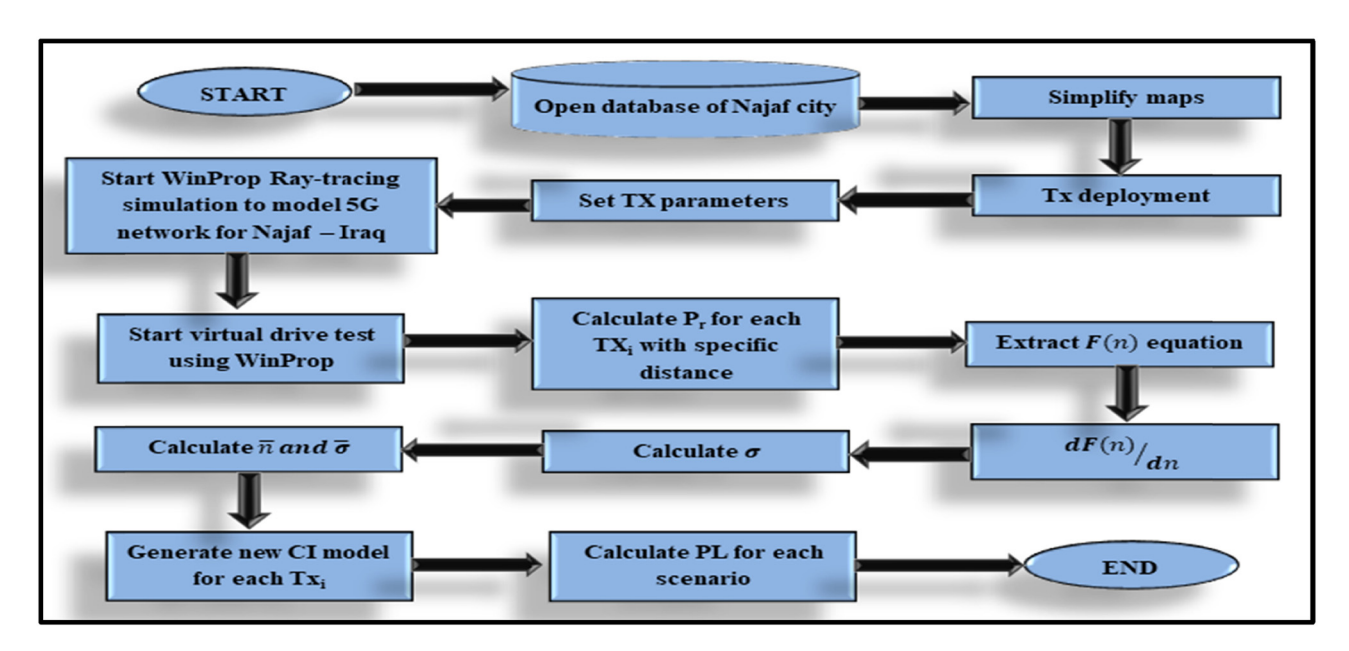
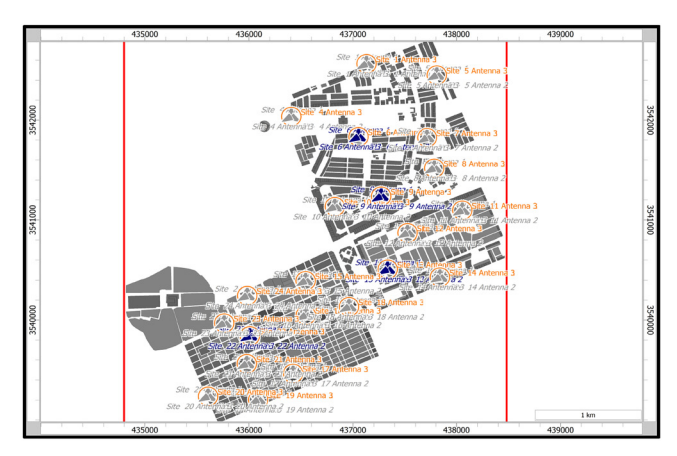
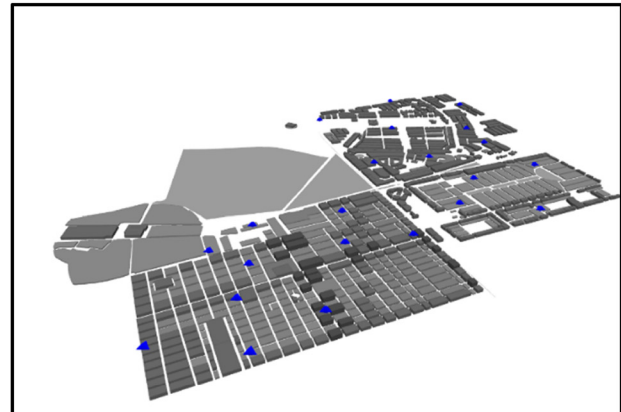


Figure 2: The study block diagram.





**Figure 3:** The available  $T_x$  towers in the targeted zone by the study.

available in the targeted zone will be calculated depending on WinProp channel simulator, as demonstrated in Figure 4. The measured values by the virtual drive test are going to be considered as real measured values of the received power. Figure 5 demonstrates both in 2D and 3D how the driving test around each site has been accomplished.

The incorporation of 3D maps of Najaf city enables a detailed representation of the urban environment, including building heights, which is crucial for accurate path loss modeling in complex urban landscapes. The use of virtual drive test simulations using WinProp software fills the gap of real 5G network measurements in Iraq, providing valuable data for path loss modeling and network optimization. The development of a modified CI path loss model tailored to the specific characteristics of Najaf city at 28 GHz provides a more accurate representation of signal propagation, considering factors like shadow fading and building obstructions.

The performance of each site is demonstrated in Figure 6 since it describes the received power as a function of distance for every transmitter available in the targeted zone. Figure 6

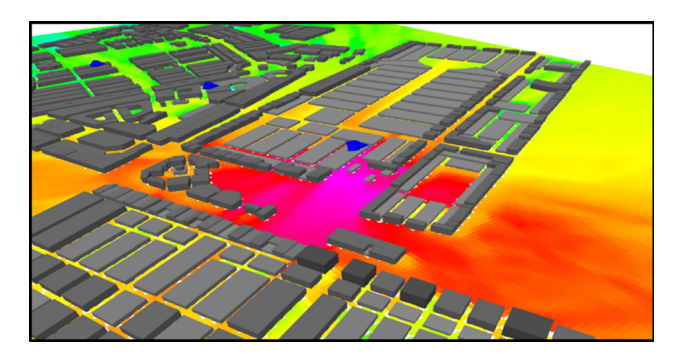
demonstrates how RSS declines with distance, especially in shadowed sites where environmental elements like structures and other obstructions in addition to free space loss are present.

In addition to outlining the experimental setup and data collection procedures, it is pertinent to discuss the computational complexity inherent in implementing the proposed model. The computational demands associated with each stage of the study play a crucial role in the feasibility and efficiency of the research endeavor.

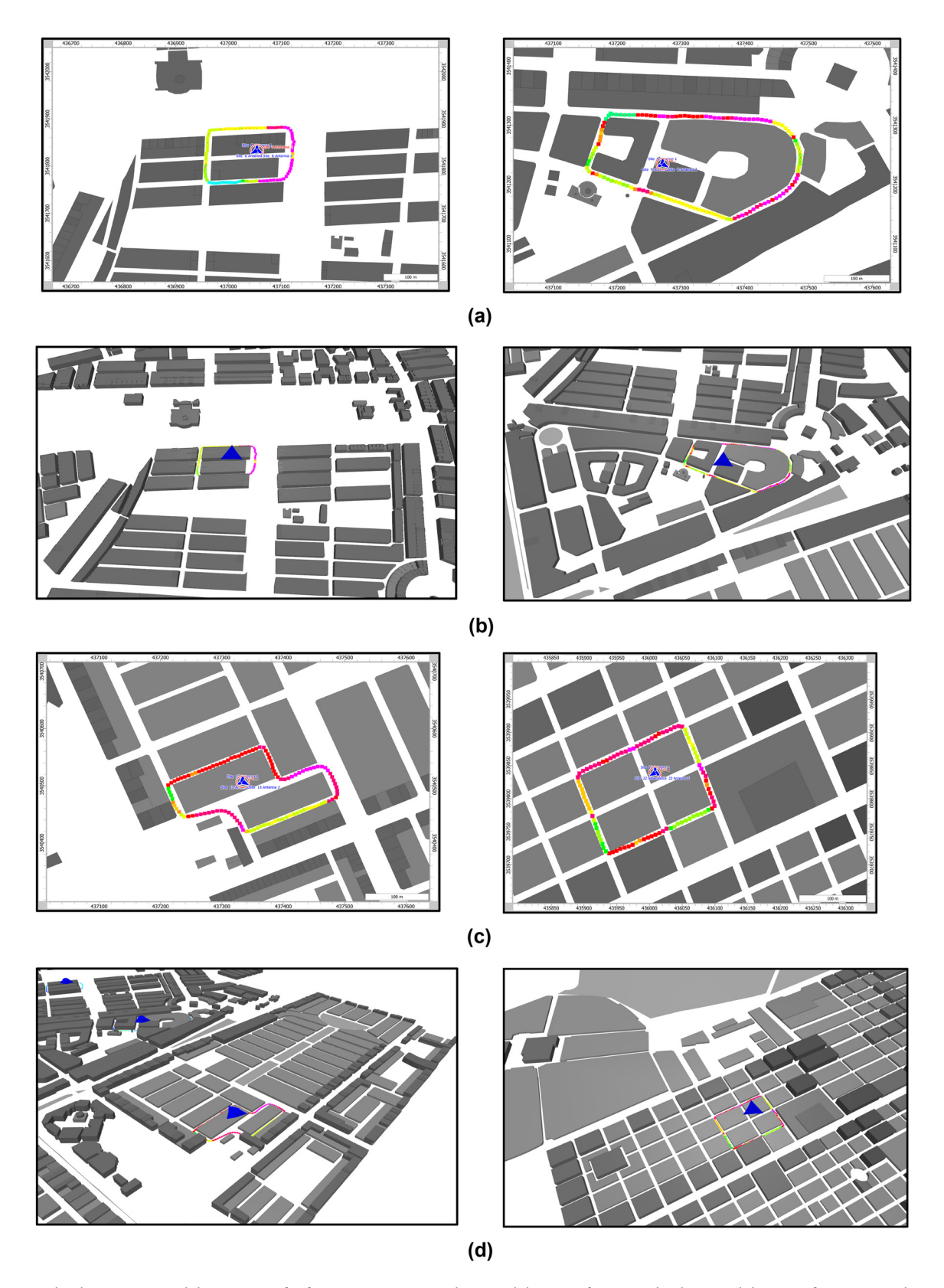
The computational complexity of the model stems from several key components. First, the conversion of 2D maps into detailed 3D representations of the urban environment requires significant computational resources, especially for large study areas such as Najaf city with intricate building structures. This process involves sophisticated algorithms for data interpolation, elevation modeling, and geometric calculations. Furthermore, executing virtual drive test simulations using WinProp software entails intensive computational tasks. These simulations involve complex ray-tracing algorithms and electromagnetic propagation models to calculate received power values for each

 Table 3: Simulation parameters of each transmitter

No.	Parameter	Value
1	Scenario	Urban Macrocell outdoor
2	Environment	NLOS
3	$T_X$ – $R_X$ distance	30-180 m
4	Frequency	28 GHz
5	Channel bandwidth	5,000 kHz
6	$T_x$ power	40 dBm
7	Bs antenna gain	15 dBi
8	BS/MS height	30-35/1.5 m
9	Antenna pattern	Directional sector
10	Antenna Azimuth	0, 120, and 240
11	Antenna Downtilt	2



**Figure 4:** The intensity of the received power for one of the deployed  $T_X$ .



**Figure 5:** The drive test around the  $T_x$  towers for four various sites. (a) The virtual drive test for site 6. (b) The virtual drive test for site 9. (c) The virtual drive test for site 13. (d) The virtual drive test for site 22.

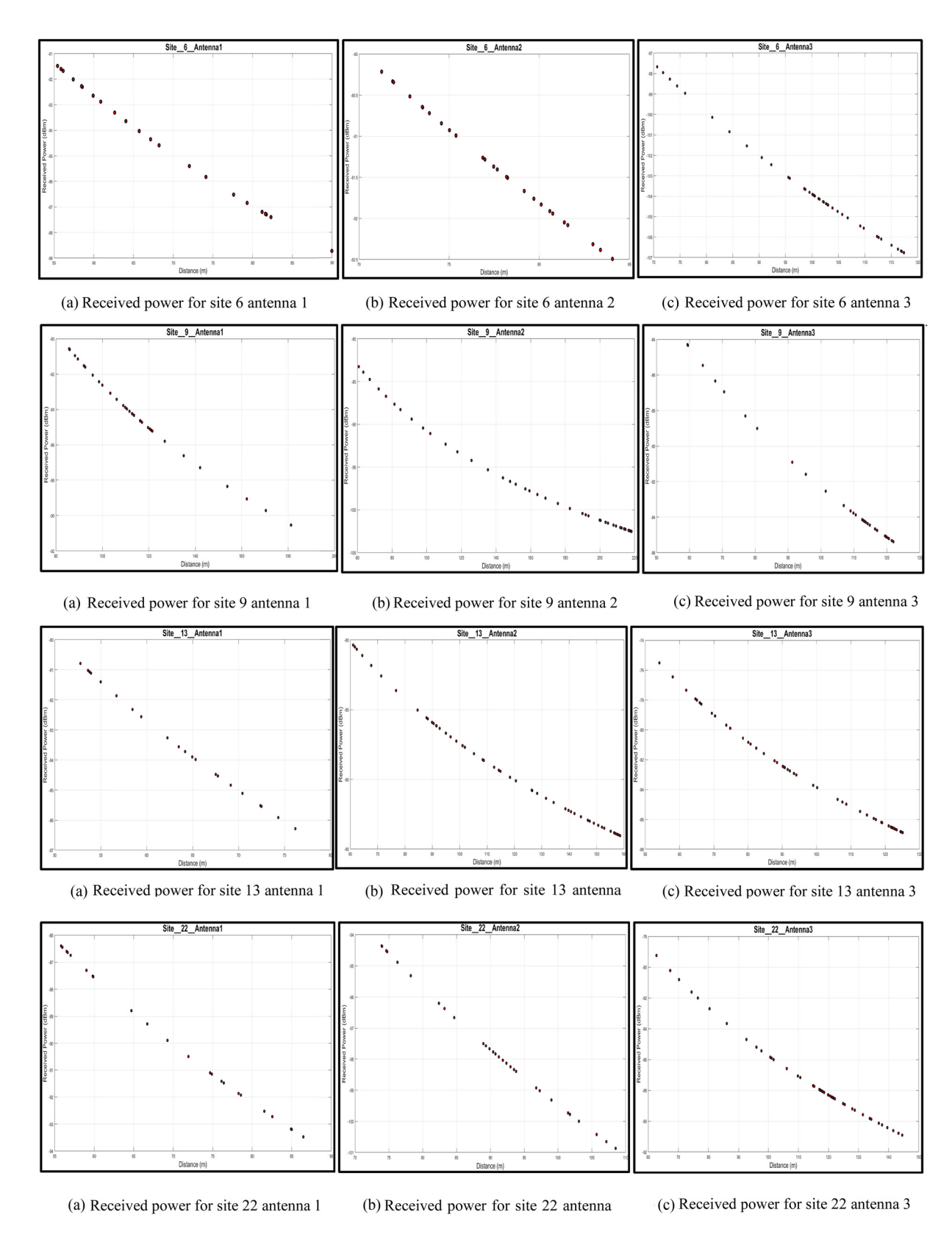


Figure 6: The received power in all sites.

transmitter at multiple locations within the study area. The high level of detail and accuracy required in these simulations further contributes to the computational complexity. Additionally, the calibration and optimization of the path loss model necessitate extensive computational resources. This involves analyzing simulation results, fitting mathematical models to observed data, and iteratively adjusting model parameters to achieve accurate predictions.

Considering multiple scenarios with different transmitter configurations and antenna patterns adds another layer of computational complexity. Each scenario requires separate simulations and analysis, increasing the overall computational workload. While the exact computational complexity metrics, such as time complexity or resource requirements, may vary depending on specific factors, such as the size of the study area and the precision of simulations, it is evident that implementing the proposed model requires substantial computational resources and efficient algorithms to manage the workload effectively.

# 4 Radio propagation model

Measuring the behavior of electromagnetic waves has allowed us to characterize their propagation, and using statistical estimates on these measurements has allowed us to build a mathematical model of their behavior. Although mathematical formulations are fairly accurate for prediction, their behavior in authentic environments is not always the same as that given by the generic theoretical model. This is due to the expression does not considering the influences of the real world. To predict the behavior of electromagnetic waves and therefore utilize them as a medium of communication, generic models are utilized in wireless communications. Subsequently, to enhance the dependability of wireless communications, it is necessary to characterize the effects in the actual world.

Because it influences the connection quality, path loss is crucial in a wireless channel. It is a measurement of how much the strength of a signal weakens between its source and its destination. Using Friis's free space equation, which is shown in 1, it is possible to make an approximation of the relationship between the transmitted and received power

$$\frac{P_{\rm r}}{P_{\rm t}}(d) = \frac{G_{\rm r}G_{\rm t}}{L} \left(\frac{\lambda}{4\pi d}\right)^2 = \frac{G_{\rm r}G_{\rm t}\lambda^2}{(4\pi)^2 d^2 L},\tag{1}$$

where  $G_t$  and  $G_r$  are the gains of the transmitting and receiving antennas, respectively,  $\lambda$  is the wavelength calculated from the system's communication frequency, d is the

separation distance between the transmitter and receiver antennas, and  $\boldsymbol{L}$  is the system loss factor that accounts for the attenuation caused by the transmission line and the losses of the antennas.

Commonly, dB is utilized to quantify the path loss. A formula may be utilized to obtain the path loss value as follows, given equation (1):

$$PL(dB) = 10 \log \left( \frac{P_t}{P_t} \right) = -10 \log \left( \frac{G_r G_t \lambda^2}{(4\pi)^2 d^2 L} \right),$$
 (2)

where  $P_t$  is the transmitter power and  $P_r$  is the receiver power.

# 5 PLE optimization

When transmitting electromagnetic waves across a wireless channel, the strength of those waves declines as the distance between the transmitter and receiver grows larger. This function calculates how much power is lost while a signal travels over a particular or several paths before reaching its destination. The rate of energy loss in both models is approximately proportional to the square of the distance traveled. The PLE factor controls the rate of decrease in this function. Equation (3) is utilized to obtain the average path loss.

$$\overline{PL}(d)[dBm] = \overline{PL}(d_0) + 10n\log\left(\frac{d}{d_0}\right), \tag{3}$$

where  $\overline{PL}$  represents the typical path loss at a certain distance d relative to some fixed reference distance  $d_0$ , and n denotes the PLE. For microcellular systems,  $d_0$  is typically measured between 1 and 100 m. Without considering the impact of shadowing, the calculation of path loss in free space is given by equation (3). Available research and empirical data suggest that, for each given distance d, the path loss PL(d) follows a log-normal distribution, defined as follows.

To calculate the exact distance between each prediction point and  $T_x$ , the following equations will be used:

$$r = \sqrt{(x_2 - x_1)^2 + (y_2 - y_1)^2},$$
 (4)

$$d = \sqrt{r^2 + (h_{\rm t} - h_{\rm u})^2},\tag{5}$$

where  $x_1$ ,  $y_1$  and  $x_2$ ,  $y_2$  denote the coordinate of the transmitter and the receiver, respectively,  $h_t$  is the transmitter elevation, and  $h_u$  is the receiver height during the drive test.

$$PL(d): N(\overline{PL}, X_{\sigma}).$$
 (6)

where  $X_{\sigma}$  denotes the Gaussian distributed random variable with zero mean and  $\sigma$  denotes standard deviation in dBm unit. When there are varying amounts of noise in the communication line, the effect of shadowing for a given transmitter and receiver may be understood using a lognormal distribution [61].

For the same set of transmitters and receivers, the lognormal distribution describes the shadowing effect as the amount of noise in the communication path varies [61]. If we rewrite equation (3) as follows, we can determine the PLE:

$$\hat{p}(d) = p(d_0) - 10n \log \left(\frac{d}{d_0}\right), \tag{7}$$

where p represents the received power in a specific distance and  $\hat{p}$  denotes the predicted power. In order to obtain the value of n, we must solve the following equation, where we minimize the mean square error of the received power and the estimated.

$$f(n) = \sum_{i=1}^{k} \left[ p_i - p_0 + 10n \log \left( \frac{d_i}{d_0} \right) \right]^2, \tag{8}$$

where k refers to the total number of separations from the source. An estimation of path loss, n, can be determined by setting the derivative of f(n) equal to zero, as demonstrated in the literature [61,62]. It is possible to calculate the standard deviation of  $X_{\sigma}$  once the path loss has been determined. To illustrate, we may write E(n) as the sum of the estimated power minus the received power. Standard deviation may be calculated as

$$E(n) = \sum_{i=1}^{k} (p_i - \hat{p}_i)^2, \tag{9}$$

$$\sigma = \sqrt{\frac{E(n)}{k}}.$$
 (10)

The values for path loss and standard deviation will fluctuate as a function of environmental variables.

# 6 Numerical results and discussion

A PLE value is utilized to describe the magnitude of the path loss as a function of the physical distance between the transmitter and receiving stations. The allowable PLE ranges from 2.7 to 3.5 dB in urban regions, 3 to 5 dB in shadowed sites, 2 dB in LoS locations, 4 to 6 dB in a blocked region with factories [18]. When the transmitter and receiver are in boresight alignment, the permissible PLE value for 28 GHz LoS mmWave is between 1.8 and 2.2 dB; conversely, it increases

to 4 and 5 dB in non-NLoS scenarios. The accomplished PLE in this study varies from 3.0619 to 4.1253 dB. To calculate the PLE from all the scenarios proposed in this research, the environment of Najaf city was utilized, and the derived PLE is within the range of acceptable PLE. The simulation has measured the received power for 423 points around all the four studied sites. Najaf city is an urban environment with high-rise buildings that cause shadowing and propagation signal obstruction. In this work, each  $T_x$  will contain three sectors. Each sector will represent a transmitting antenna that propagates the signal within various azimuth angles of the other antenna in the same  $T_{\rm r}$ . Four  $T_{\rm r}$  will be investigated with three transmitters for each  $T_x$  making 12 various scenarios will be discussed during the study. Using equation (1) through equation (8), as mentioned in the preceding section, the CI model has been utilized to represent the path loss model, as detailed in the studies of Maccartney and Member [37] and Li et al. [45]. Table 4 reflects how we utilize this assumption to develop a better path loss model by averaging the results of the several simulation scenarios and then expressing  $T_{x_1}$ ,  $T_{x_2}$ , and  $T_{x_3}$  for each site as a single number. Equation (9) is derived by fitting a regression model to the average values of n and  $X_{\sigma}^{CI}$  in a CI model

$$PL^{CI}(f, d)[dB] = FSPL(f, d_0)[dB] + 10n \log_{10}(d) + X_{\sigma}^{CI},$$
 (11)

where  $d_0$  is the CI free space reference distance in m, n is the PLE, and  $X_{\sigma}^{\text{CI}}$  is the shadow fading with a zero-mean Gaussian random variable and standard deviation  $\sigma$ ; furthermore, FSPL is the free space path loss. To generate a new CI path loss model for Najaf city at 28 GHz, we substitute the calculated CI parameters into equation (11). Average path loss for  $T_x$  locations, denoted by PL(d) dB from equations (12) to (23).

Site 6 contains three separated antennas with various azimuth angles (0, 120, and 240). Each  $T_x$  will share the same coordinate and elevation of the site, which is X=437054.56, Y=3541833.08, Z=30. Based on the recorded results of the CI model parameters n and  $X_{\sigma}^{\text{CI}}$ , a new equation for each  $T_x$  will be generated. The calculated path loss for each  $T_x$ , the recorded PLE, and the standard

**Table 4:** Key path loss model parameters and the recorded average path loss

$T_X$	$T_X$ – $R_X$ average (m)	Average calculated PL (dB)	σ	n
$T_{x_1}$	69.757	128.430609	3.9202	3.4462
$T_{x_2}$	77.346	127.017059	5.6867	3.1751
$T_{x_3}$	99.65157	150.4943903	6.8265	4.1253

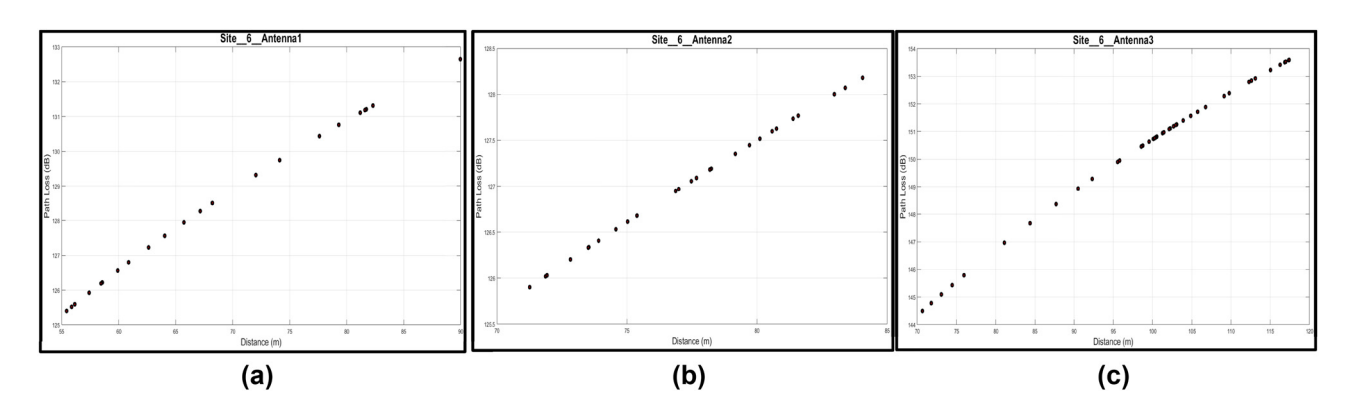


Figure 7: Calculated path loss for site 6 using the modified CI model. (a) Path loss for site 6 antenna 1, (b) path loss for site 6 antenna 2, and (c) path loss for site 6 antenna 3.

deviation are illustrated in Table 4. Figure 7 demonstrates the calculated path loss as a function of distance for the three sectors available in site 6

$$PL_{S6-T_{x_1}} = 135.0489 \log_{10}(d),$$
 (12)

$$PL_{S6-T_{x_2}} = 150.0029 \log_{10}(d),$$
 (13)

$$PL_{S6-T_{x_3}} = 170.9029 \log_{10}(d).$$
 (14)

Based on the same procedures that are utilized on site 6, the equations of the modified CI path loss model related

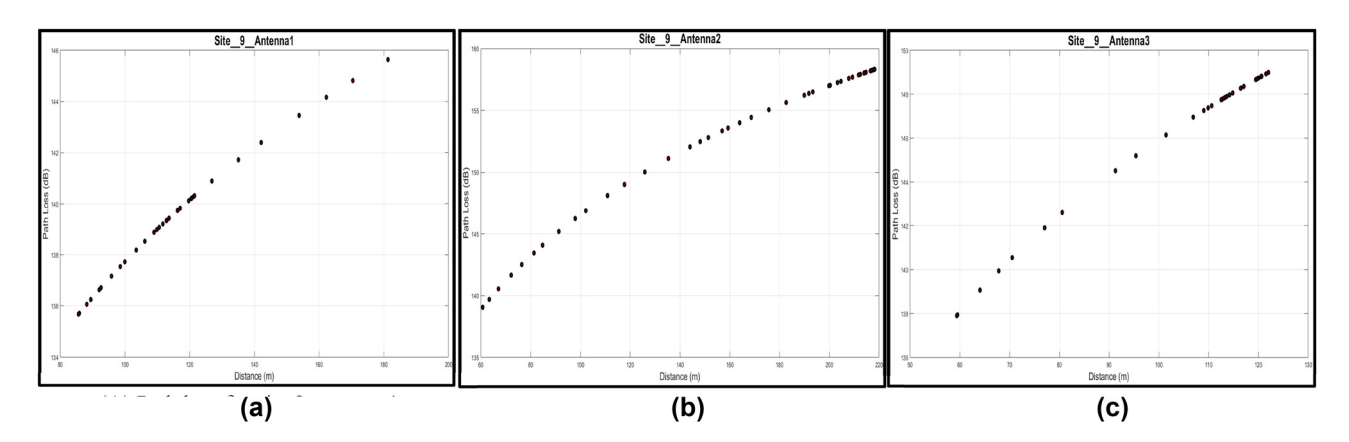


Figure 8: Calculated path loss for antenna available in site 9. (a) Path loss for site 9 antenna 1, (b) path loss for site 9 antenna 2, and (c) path loss for site 9 antenna 3.

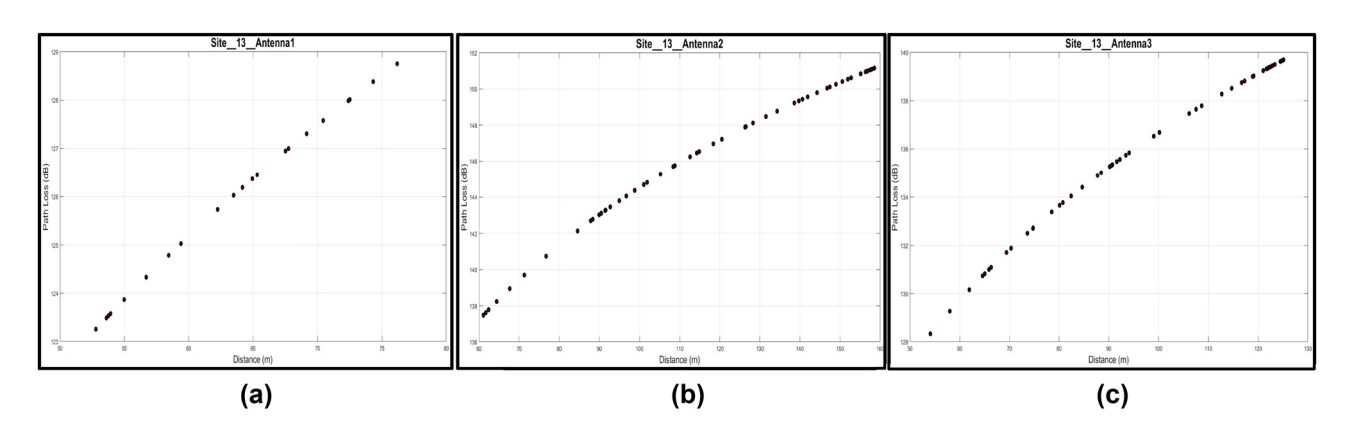


Figure 9: Calculated path loss for the antenna available in site 13. (a) Path loss for site 13 antenna 1, (b) path loss for site 13 antenna 2, and (c) path loss for site 13 antenna 3.

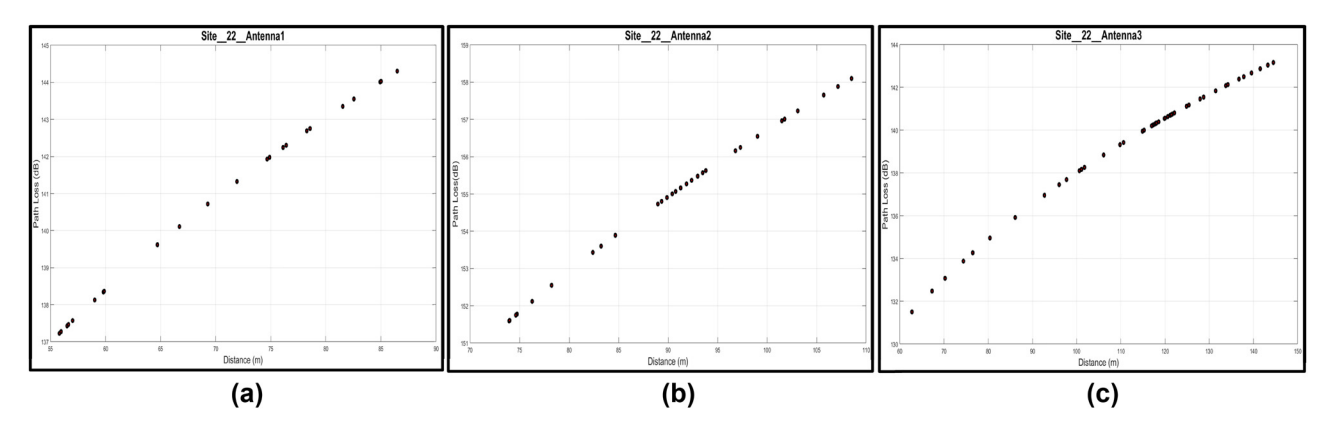


Figure 10: Calculated path loss for the antenna available in site 22. (a) Path loss for site 22 antenna 1, (b) path loss for site 22 antenna 2, and (c) path loss for site 22 antenna 3.

to site 9 will be generated. The coordinate of site 9 is X =437271.31, Y = 3541234.63, Z = 30.

$$PL_{S9-T_{x_1}} = 243.0499 \log_{10}(d),$$
 (15)

$$PL_{S9-T_{X2}} = 254.0899 \log_{10}(d),$$
 (16)

$$PL_{S9-T_{r_2}} = 232.9509 \log_{10}(d).$$
 (17)

The obtained equations for site 13 (X = 437334.01, Y =3540506.91, Z = 30) based on the averaging of CI path loss model's parameters are denoted by equations (18)-(20).

$$PL_{S13-T_{x_1}} = 120.5729 \log_{10}(d),$$
 (18)

$$PL_{S13-T_{v_2}} = 265.6129 \log_{10}(d),$$
 (19)

$$PL_{S13-T_{v_2}} = 220.7359 \log_{10}(d).$$
 (20)

The following equations have been utilized for calculating the value of path loss for site 22 (X = 436008.73, Y =3539839.44, Z = 35) based on the new CI model.

$$PL_{S22-T_{X_1}} = 206.8699 \log_{10}(d),$$
 (21)

$$PL_{S22-T_{x_2}} = 272.7629 \log_{10}(d),$$
 (22)

$$PL_{S22-T_{x_3}} = 216.1929 \log_{10}(d).$$
 (23)

Figures 7-10 show the correlation of the increase in the value of path losses at 28 GHz in conjunction with the increase in the separating distance between the transmitter and the receiver. When comparing the PLE obtained from this study, which ranges between 3.0619 and 4.1253, with the value of the FSPL exponent, which is equal to 2, we find that the difference between the two measurements occurred because of the obstacles between the transmitter and the receiver. The standard deviation values range between 2.4703 and 17.2331. This change in values is due to the different distribution and types of buildings within the transmission medium, which causes various shadowing effects for all scenarios (Tables 5-7).

Comparing the accomplished path loss model in this study with some models accomplished by researchers [18,43,63,64,65], the accomplished model reflected its advantage. The PLE values recorded by this work are between 3.0619 and 4.1253. For the scenario of path loss

Table 6: Key path loss model parameters and the recorded average path loss

$T_{x}$	$T_x$ $R_x$ average (m)	Average calculated PL (dB)	σ	n
$T_{x_1}$	63.53119567	125.9326434	2.4703	3.4485
$T_{x_2}$	114.9022571	145.9929742	17.1208	3.3020
$T_{x_3}$	95.31542161	135.6185297	12.8121	3.1230

Table 5: Key path loss model parameters and the recorded average path loss

$T_{x}$	$T_X$ $R_X$ average (m)	Average calculated PL (dB)	σ	n
$T_{x_1}$	115.5865382	139.4032136	15.1046	3.0619
$T_{x_2}$	159.2926146	152.4995947	15.8019	3.4686
$T_{x_3}$	101.6089596	145.7665808	13.6100	3.5466

Table 7: Key path loss model parameters and the recorded average path loss

$T_X$	$T_X$ $R_X$ average (m)	Average calculated PL (dB)	σ	n
$T_{x_1}$	70.11916057	140.7263272	10.8265	3.7220
$T_{x_2}$	90.66635187	154.9456395	17.2331	3.9047
$T_{x_3}$	113.4382247	139.5246479	12.2623	3.2185

with and without antenna pattern Hinga and Member [18], accomplished PLE values equal to 3.8 and 3.98 in  $T_{x3}$  and  $T_{x4}$ , whereas the average PLE recorded in this study for sites 13 and 22 equal to 3.29 and for site 3 3.61. Hinga and Member [18] recorded a maximum shadow factor of 93.5 for the scenario of path loss with and without antenna pattern, while this study has recorded a maximum shadow factor equal to 17.2331. Environment [65] and Adegoke et al. [43] recorded PLE values of 4.3202 and 4.214 for the V-V and V-H configurations and 4.74, respectively, which are in excess of the maximum PLE value recorded by this study. Zhang et al. [63] recorded 5.76 PLE value for 28 GHz, whereas this study recorded less value. Maccartney et al. [64] recorded 3.6 PLE for NLOS 28 GHz, whereas this study recorded an average PLE less than this value for all the simulated sites.

#### 7 Conclusion

Calibration and tuning are required for the scenario of a field campaign in mmWave band large-scale path loss modeling. The authors of this study have utilized the WinProp intelligent ray tracing, Feko, to simulate a 5G communication testbed for the city of Najaf in Iraq, utilizing a deterministic 3D ray-tracing approach. No previous work of this kind has been done at 28 GHz in the study region; hence, the findings of this study will be of interest to researchers and 5G communication service providers planning to conduct pilot studies or actual implementations. Shadow fading has a significant impact on path loss models in densely populated metropolitan places like Najaf city; therefore, studying its effects is crucial. As compared to previous studies conducted at 28 GHz, the shadow factor reported in our model is an ameliorated model. This framework can serve as a reference for mmWave band researchers concentrating on Najaf City, and it can be adjusted for utilizing in other locations. A genuine LoS and NLoS field campaign at 28 GHz is anticipated for future research. Ongoing research and industry efforts are advancing path loss modeling for 5G networks, particularly in urban environments. Leveraging technologies such as AI, mmWave communications, and network slicing, researchers aim to improve coverage, capacity, and reliability. AI-driven approaches enable precise propagation modeling, while mmWave research focuses on beamforming and channel estimation. Additionally, green communication initiatives promote sustainability and efficiency in network design. Collaborative efforts between academia and industry are crucial for realizing the full potential of 5G connectivity. A

similar investigation will be carried out in all of Iraq's provinces for the purpose of generating an accurate path loss model.

Conflict of interest: Authors state no conflict of interest.

**Data availability statement:** Most datasets generated and analyzed in this study are in this submitted manuscript. The other datasets are available on reasonable request from the corresponding author with the attached information.

#### References

- [1] Talib M, Aripin NBM, Othman NS, Sallomi AH. Comprehensive overview on millimeter wave communications for 5G networks concentrating on propagation models for different urban environments. J Phys Conf Ser. 2022;2322(1):1–23. doi: 10.1088/1742-6596/2322/1/012095.
- [2] Erunkulu OO. Cellular communications coverage prediction techniques: a survey and comparison. IEEE Access. 2020;8:113052–77. doi: 10.1109/ACCESS.2020.3003247.
- [3] Rappaport TS, Sun S, Mayzus R, Zhao H, Azar Y, Wang K, et al. Millimeter wave mobile communications for 5G cellular: It will work! IEEE Access. 2013;1:335–49. doi: 10.1109/ACCESS.2013. 2260813
- [4] Koymen OH, Partyka A, Subramanian S, Li J, Sounder AC. Indoor mm-Wave Channel Measurements: Comparative Study of 2. 9 GHz and 29 GHz. 2015 IEEE Global Communications Conference (GLO-BECOM); 2015. p. 7–12.
- [5] Chen WC. 5G mmWAVE technology design challenges and development trends. 2020 International Symposium on VLSI Design, Automation and Test (VLSI-DAT); 2020. p. 15–8.
- [6] Mao X, Jin J, Yang J. Wireless channel modeling methods: classification. Comp Appl. 2010;1669–73.
- [7] Luebbers R. Propagation prediction for hilly terrain using GTD wedge diffraction. IEEE Trans Antennas Propag. 1984;9:951–5.
- [8] Hufford GA. An integral equation approach to the problem of wave propagation over an irregular surface. Q Appl Math. 1952;2:391–404.
- [9] Shishegar VMAA. Modified wavefront decomposition method for fast and accurate ray-tracing simulation. IET Microwaves, Antennas Propaq. October 2011;6:295. doi: 10.1049/iet-map.2011.0264.
- [10] Zelley CA, Constantinou CC. A three-dimensional parabolic equation applied to VHF/UHF propagation over irregular terrain. IEEE Trans Antennas Propag. 1999;47(10):1586–96.
- [11] Vehicular TON. Empirical formula for propagation loss in land mobile radio services. IEEE Trans Veh Technol. 1980;V(3):317–25.
- [12] Popoola SI, Oseni OF. Performance evaluation of radio propagation models on GSM network in Urban Area of Lagos, Nigeria. Int J Sci Eng Res. 2014;5(6):1212–7.
- [13] Andreev RVAAV. COST 231 Hata adaptation model for urban conditions in LTE networks. 2016 17th International Conference of Young Specialists on Micro/Nanotechnologies and Electron Devices (EDM); 2016. p. 64–6.
- [14] Cheerla S, Ratnam DV, Dabbakuti JRKK. An Optimized path loss model for urban wireless channels, in microelectronics,

- electromagnetics and telecommunications. Lecture Notes in Electrical Engineering. Springer: Singapore; p. 293-301. doi: 10. 1007/978-981-15-3828-5.
- [15] Al-shuwaili A. 5G channel characterization at millimeter-wave for Baghdad City: An NYUSIM-based Approach, in 2021 18th International Multi-Conference on Systems. Signals & Devices; 2021. p. 468-73. doi: 10.1109/SSD52085.2021.9429348.
- [16] Jamel TM. Optimum and Appropriate 5G Millimeter Wave Frequencies for Baghdad City. The 3rd Conference of Post Graduate Researches & Graduation Projects CPGR'2021; 2021.
- [17] Rappaport TS, MacCartney GR, Samimi MK, Sun S. Wideband millimeter-wave propagation measurements and channel models for future wireless communication system design. IEEE Trans Commun. 2020;63(9):3029-56. doi: 10.1109/TCOMM.2015.2434384.
- [18] Hinga SK, Member GS. Deterministic 5G mmWave large-Scale 3D path loss model for Lagos Island, Nigeria. IEEE Access. 2021;9. 134270-88. doi: 10.1109/ACCESS.2021.3114771.
- [19] Phillips C, Sicker D, Grunwald D. A Survey of wireless path loss prediction and coverage mapping methods. IEEE Commun Surv Tutor. 2013;15(1):255-70.
- [20] Al-samman AM, Rahman TA, Hindia MHDN, Daho A. Path Loss model for outdoor parking environments at 28 GHz and 38 GHz for 5G wireless networks. Symmetry (Basel). 2018;10:672. doi: 10.3390/sym10120672.
- Popoola SI, Atayero AA, Popoola OA. Data in brief comparative assessment of data obtained using empirical models for path loss predictions in a university campus environment. Data Br. 2018;18:380-93. doi: 10.1016/j.dib.2018.03.040.
- [22] Shehzad K, Khan NM, Ahmed J. Performance analysis of coveragecentric heterogeneous cellular networks using dual-slope path loss model. Comput Networks. October 2020;185:107672. doi: 10.1016/j. comnet.2020.107672.
- [23] Al-samman AM, Rahman TA, Azmi MH, Hindia MN. International Journal of Electronics and Communications (AEÜ) Large-scale path loss models and time dispersion in an outdoor line-of-sight environment for 5G wireless communications. AEUE - Int J Electron Commun. 2016;70(11):1515-21. doi: 10.1016/j.aeue.2016.09.009.
- [24] Elizabeth FQ, Grøtli EI, Johansen TA. Task assignment for cooperating UAVs under radio propagation path loss constraints. 2012 American Control Conference (ACC), IEEE; 2012, p. 3278-83.
- [25] Anusha VS, Nithya GK, Rao SN. A comprehensive survey of electromagnetic propagation models. 2017 International Conference on Communication and Signal Processing (ICCSP); 2017. p. 1457–62.
- [26] Sarkar TK, Abdallah MN, Salazar-palma M. Survey of available experimental data of radio wave propagation for wireless transmission. IEEE Trans Antennas Propag. 2018;66(12):6665-72.
- [27] Sasidhar K. A survey based analysis of propagation models over the sea. 2015 International Conference on Advances in Computing, Communications and Informatics (ICACCI). Kochi, India: IEEE; 2015.
- [28] Hrovat A, Kandus G, Member S. A survey of radio propagation modeling for tunnels. 2014;16(2):658-69. doi: 10.1109/SURV.2013.
- [29] Ahmadien O, Ates HF, Member S. Predicting path loss distribution of an area from satellite images using deep learning. IEEE Access. 2020;8:64982-91. doi: 10.1109/ACCESS.2020.2985929.
- [30] Wu L, Member S, He D. Artificial neural network based path loss prediction for wireless communication network. IEEE Access. 2020;8:199523-38. doi: 10.1109/ACCESS.2020.3035209.
- [31] Ates HF, Member S, Hashir SM. Path loss exponent and shadowing factor prediction from satellite images using deep learning. IEEE Access. 2019;7:101366-75.

- [32] Seidel SY, Rappaport TS. A ray tracing technique to predict path loss and delay spread inside. GLOBECOM '92 - Communications for Global Users. IEEE; 1992. p. 2-6.
- [33] Charitos M et al. LTE-A virtual drive testing for vehicular environments. 2017 IEEE 85th Vehicular Technology Conference (VTC Spring); 2017. p. 2-6.
- [34] Thrane J, Member S, Zibar D. Model-aided deep learning method for path loss prediction in mobile communication systems at 2. 6 GHz. IEEE Access. 2020;8:7925-36.
- [35] Han SY, Abu-ghazaleh NB, Lee D. Efficient and consistent path loss model for mobile network simulation. IEEE/ACM Trans Netw. 2016;24(3):1774-86.
- Ju S, Kanhere O, Xing Y, Rappaport TS. A millimeter-wave channel simulator NYUSIM with spatial consistency and human blockage. 2019 IEEE Glob Commun Conf GLOBECOM 2019 - Proc; 2019. p. 1-6. doi: 10.1109/GLOBECOM38437.2019.9013273.
- [37] Maccartney GR, Member S. Indoor office wideband millimeterwave propagation measurements and channel models at 28 and 73 GHz for ultra-dense 5G wireless networks. IEEE Access. 2015;3. 2388-24. doi: 10.1109/ACCESS.2015.2486778.
- Sun S, Rappaport TS, Thomas TA, Ghosh A, Nguyen HC, Kovacs IZ, et al. Investigation of prediction accuracy, sensitivity, and parameter stability of large-scale propagation path loss models for 5G wireless communications. IEEE Trans Veh Technol. 2016;65(5):2843-60. doi: 10.1109/TVT.2016.2543139.
- Bhuvaneshwari A, Hemalatha R, Satyasavithri T. Semi deterministic [39] hybrid model for path loss prediction improvement. Procedia -Procedia Comput Sci. 2016;92:336-44. doi: 10.1016/j.procs.2016.07.388.
- [40] Al-samman AM, Azmi MH, Al-hadhrami T. Millimeter wave propagation measurements and characteristics for 5G system. Appl Sci. 2019;10:1-17.
- Al-samman AM, Rahman TA, Al-hadhrami T. Comparative study of indoor propagation model below and above 6 GHz for 5G wireless networks. Electronics. 2019;8:1-26. doi: 10.3390/8010044.
- [42] Adegoke EI, Kampert E, Higgins MD. Empirical indoor path loss models at 3. 5GHz for 5G communications network planning; 2020. p. 1-4.
- [43] Adegoke EI, Kampert E, Higgins MD, Member S. Channel modeling and over-the-air signal quality at 3. 5 GHz for 5G new radio. IEEE Access. 2021;9:11183-93. doi: 10.1109/ACCESS.2021.3051487.
- [44] Al-samman AM, Rahman TA, Azmi MH, Sharaf A, Yamada Y, Alhammadi A. Path loss model in indoor environment at 40 GHz for 5G wireless network. 2018 IEEE 14th International Colloquium on Signal Processing & Its Applications (CSPA). Penang, Malaysia: IEEE; 2018. p. 9-10.
- [45] Li S, Liu Y, Lin L, Sun D, Yang S, Sun X. Simulation and modeling of millimeter-wave channel at 60 GHz in indoor environment for 5G wireless communication system. 2018 IEEE International Conference on Computational Electromagnetics (ICCEM). IEEE; 2018. p. 5-7.
- Jr GRM, Rappaport TS, Samimi MK, Sun S. Millimeter wave omnidirectional path loss data for small cell 5G channel modeling. IEEE Access. Vol. 3536, 2015. doi: 10.1109/ACCESS.2015. 2465848.
- [47] Lee J, Liang J, Kim M, Park J, Park B, Chung HK. Measurement-based propagation channel characteristics for millimeter-wave 5G giga communication systems. ETRI J. 2016;38(6):1031-41.
- Kuno N, Yamada W, Sasaki M, Taratori Y. Convolutional neural network for prediction method of path loss characteristics considering diffraction and reflection in an open-square environment.

- 2019 URSI Asia-Pacific Radio Sci Conf AP-RASC 2019; 2019. p. 4–6. doi: 10.23919/URSIAP-RASC.2019.8738299.
- [49] Chunyu Ge XJ, Zhang Y. Simulation and analysis of 28GHz millimeter-wave propagation characteristics in typical residential house environment. 11th UK-Europe-China Workshop on Millimeter Waves and Terahertz Technologies (UCMMT); 2018. p. 7–9.
- [50] Kitao K, Benjebbour A, Imai T, Kishiyama Y, Inomata M, Okumura Y. 5G system evaluation tool. in 2018 IEEE International workshop on electromagnetics: Applications and student innovation competition (iWEM). IEEE; 2018. p. 30–1.
- [51] Hossain F, Geok T, Rahman T, Hindia M, Dimyati K, Ahmed S, et al. An efficient 3-D ray tracing method: prediction of indoor radio propagation at 28 GHz in 5G network. Electron. 2019;8:286. doi: 10. 3390/electronics8030286.
- [52] Yang C, Ieee M, Wu B, Ko C. A ray-tracing method for modeling indoor wave propagation and penetration. IEEE Trans Antennas Propag. 1998;46(6):907–19.
- [53] Modeling IP, Introduction I, Tooth B, Pilot P. Efficient implementation of deterministic 3-D ray tracing model to predict propagation losses in indoor environments. The 13th IEEE International Symposium on Personal, Indoor and Mobile Radio Communications; 2002.
- [54] Díaz W. A path loss simulator for the 3GPP 5G channel models. 2018 IEEE XXV International Conference on Electronics, Electrical Engineering and Computing (INTERCON); 2018. p. 7–10.
- [55] Dupleich D, Abbas Mir H, Schneider C, Del Galdo G, Thoma R. On the modelling of the NLOS first multi-path component in stochastic spatial channel models. 15th Eur Conf Antennas Propagation, EuCAP 2021; 2021. doi: 10.23919/EuCAP51087.2021.9411142.
- [56] Major International 5G Trials and Pilots 5G Observatory. https:// 5gobservatory.eu/5g-trial/major-international-5g-trials-and-pilots/ (accessed Feb. 15, 2023).

- [57] Lubke M, Dimce S, Schettler M, Lurz F, Weigel R, Dressler F. Comparing mmWave channel simulators in vehicular environments. IEEE Veh Technol Conf; 2021-April. doi: 10.1109/VTC2021-Spring51267.2021.9448732.
- [58] Krause A, Anwar W, Martinez AB, Stachorra D, Fettweis G, Franchi N. Network planning and coverage optimization for mobile campus networks. Proc – 2021 IEEE 4th 5G World Forum, 5GWF 2021; 2021, p. 305–10. doi: 10.1109/5GWF52925.2021.00060.
- [59] Hoppe R, Wolfle G, Jakobus U. Wave propagation and radio network planning software WinProp added to the electromagnetic solver package FEKO. 2017 Int Appl Comput Electromagn Soc Symp – Italy, ACES 2017; 2017. p. 3–4. doi: 10.23919/ROPACES.2017.7916282.
- [60] Ußler H, Setzefand C, Kanis D, Schwarzbach P, Michler O. Efficient coverage planning for full-area C-ITS communications based on radio propagation simulation and measurement tools. 27th ITS World Congress; 2021. p. 11–5.
- [61] Miranda J et al. Path loss exponent analysis in wireless sensor networks: Experimental evaluation. IEEE Int Conf Ind Informatics; 2013. p. 54–8 doi: 10.1109/INDIN.2013.6622857.
- [62] Nsaif BG, Sallomi AH. Path loss modeling for urban wirless networks in Baghdad. J Eng Sustain Dev. 2021;25:1–7. doi: 10.31272/ jeasd.conf.2.1.2.
- [63] Jr GRM, Zhang J, Nie S, Rappaport TS. Path loss models for 5G millimeter wave propagation channels in urban microcells. 2013 11th IEEE International Conference on Industrial Informatics (INDIN). IEEE; 2013. p. 3948–53.
- [64] Maccartney GR, Rappaport TS, Samimi MK, Sun SHU. Millimeter-wave omnidirectional path loss data for small cell 5G channel modeling. IEEE Access. 2015;3:1573–80. doi: 10.1109/ACCESS.2015.2465848.
- [65] Environment O. Investigation of future 5G-IoT millimeter-wave network performance at 38 GHz for Urban microcell. Electron. 2019.